



Research Article

A New Model-Free Trajectory Tracking Control for Robot Manipulators

Yaoyao Wang ^{1,2}, Kangwu Zhu,³ Bai Chen ¹ and Hongtao Wu¹

¹College of Mechanical and Electrical Engineering, Nanjing University of Aeronautics and Astronautics, Nanjing 210016, China

²State Key Laboratory of Fluid Power and Mechatronic Systems, Zhejiang University, Hangzhou 310027, China

³Shanghai Institute of Spaceflight Control Technology, Shanghai 200233, China

Correspondence should be addressed to Yaoyao Wang; yywang_cmee@nuaa.edu.cn

Received 17 September 2018; Revised 14 November 2018; Accepted 29 November 2018; Published 30 December 2018

Academic Editor: Libor Pekař

Copyright © 2018 Yaoyao Wang et al. This is an open access article distributed under the Creative Commons Attribution License, which permits unrestricted use, distribution, and reproduction in any medium, provided the original work is properly cited.

In this paper, we propose a novel model-free trajectory tracking control for robot manipulators under complex disturbances. The proposed method utilizes time delay control (TDC) as its control framework to ensure a model-free scheme and uses adaptive nonsingular terminal sliding mode (ANTSM) to obtain high control accuracy and fast dynamic response under lumped disturbance. Thanks to the application of adaptive law, the proposed method can ensure high tracking accuracy and effective suppression of noise effect simultaneously. Stability of the closed-loop control system is proved using Lyapunov method. Finally, the effectiveness and advantages of the newly proposed TDC scheme with ANTSM dynamics are verified through several comparative simulations.

1. Introduction

Robot manipulators have been widely used in lots of fields due to their strong capacity to realize all kinds of automatic working tasks [1, 2]. Usually, high performance trajectory tracking control of robot manipulators is required to execute the tasks, which, however, is still an open challenging job [3, 4]. The main difficulties can be concluded as strong nonlinearities, large couplings and unknown lumped time-varying disturbances [5].

To ensure good control performance under lumped complex uncertainties, lots of scholars have devoted themselves in this field and proposed some effective methods. In [6], a novel continuous finite time control scheme was proposed for uncertain robot manipulators using integral sliding mode (SM) dynamics. Good control performance has been observed through simulation studies. In [7], a novel control/identification algorithm was proposed and investigated for the high performance control of robot manipulators. By properly integrating the parametric estimation error information into the designed identification scheme, high comprehensive performance has been obtained. In [8], a new

model predictive control (MPC) was proposed using integral sliding mode (ISM) dynamics. Thanks to the effective combination of MPC and ISM schemes, satisfactory comprehensive control performance has been obtained with the proposed control scheme. In [9], a novel adaptive fuzzy control scheme was proposed for the position/force tracking control purpose of cooperative robot manipulators. By using the fuzzy logic to estimate the unknown system dynamics and adaptive control to ensure high control accuracy, the designed control scheme can ensure good comprehensive control performance. To ensure high accuracy trajectory tracking control performance of robot manipulators, a novel adaptive fuzzy neural network control scheme was proposed and studied [10]. Other control schemes have also been proposed and investigated for the control purpose of complex systems [11–13]. Despite the exiting results obtained with the above-mentioned control schemes, they are usually not suitable for complicated real situations due to the requirement of system dynamic model or complex estimation algorithms.

As a well-known model-free control scheme, time delay control (TDC) can efficiently solve the above issues in a simple way [14–20]. The core element of TDC scheme is

the so-called time delay estimation (TDE), which uses the time-delayed values of the system states to estimate the remaining system dynamics and ensures a model-free feature. Thanks to the above attractive feature, TDC control has been widely used in lots of systems [21–27]. By combining TDE with other robust control schemes, exciting results have been obtained. In [28], a novel TDC scheme was proposed for the trajectory tracking control of underwater vehicles. The proposed method used TDE to estimate the system lumped dynamics and then applied PD-type error dynamics to ensure desired dynamics. Afterwards, an improved scheme based on discrete TDE (DTDE) was reported, which effectively suppressed the noise effect [29]. Still, linear error dynamics was utilized in [29]. In [30], the artificial bee colony (ABC) algorithm was used to further enhance the TDC scheme. Obvious control performance improvement has been clearly observed with the above-mentioned TDC scheme with ABC algorithm. To further improve the control performance, a novel TDC scheme with terminal sliding mode (TSM) was proposed and investigated for the robot manipulators [17]. The proposed method utilizes TDE to obtain the system dynamics and applied TSM error dynamics to guarantee high control accuracy. Thanks to the attractive finite time convergence nature and high performance near the equilibrium point, TSM control has been widely used in many systems [31–41]. Recently, a novel continuous NTSM (CNTSM) scheme has been proposed and investigated for the control purpose of robot manipulators [42, 43]. Exciting results have been reported in [42, 43], which effectively verified the validity of both TDE scheme and NTSM error dynamics. Still, the control scheme proposed in [42, 43] can be further improved. The well-known fast-TSM-type reaching law with constant parameters was used, which may be not suitable for complicated real situations. When external disturbance appears, we need extra robust term to suppress it and maintain good control performance. When external disturbance disappears, the extra robust term should also go to suppress the chattering problem. The above expectation can hardly realize using the fast-TSM-type reaching law with constant parameters. To maintain good control performance throughout the control process, sufficiently large constant parameters are obligatory, which, however, may lead to unwanted chattering and control performance degradation.

To effectively settle the above issues, we propose a novel TDC scheme with ANTSM dynamics for the robot manipulators in this work. The proposed method utilizes TDC as its basic control framework and ensures an attractive model-free nature. Afterwards, the NTSM error dynamics together with a combined reaching law are used to provide with high control accuracy and fast dynamic response and strong robustness. Stability of the closed-loop control system is analyzed using Lyapunov method. Finally, comparative simulations were conducted to demonstrate the effectiveness and advantages of our newly proposed method over the existing TDC schemes with NTSM error dynamics.

The contributions we try to make in this paper can be given as follows:

(1) Propose a new TDC scheme using ANTSM dynamics. Using a combined adaptive reaching law and the NTSM

dynamics, we propose a novel TDC scheme which can ensure good comprehensive control performance.

(2) Present the stability analysis of the closed-loop control system considering the ANTSM dynamics.

(3) Verify the effectiveness and superiorities of our newly proposed TDC scheme over the existing methods by several comparative simulation studies.

The rest is organized as what follows. Section 2 presents the main results and gives the proposed control scheme design. Section 3 gives the stability analysis using Lyapunov method; meanwhile, Section 4 demonstrates the validity of the proposed method through comparative simulation studies. Finally, Section 5 concludes this paper.

2. TDC Scheme Design with ANTSM

2.1. System Modeling. The robot manipulators with n -DOFs can be described by the following equation [17]:

$$\mathbf{M}(\mathbf{q}) \ddot{\mathbf{q}} + \mathbf{C}(\mathbf{q}, \dot{\mathbf{q}}) \dot{\mathbf{q}} + \mathbf{G}(\mathbf{q}) + \mathbf{Fr}(\mathbf{q}, \dot{\mathbf{q}}) + \boldsymbol{\tau}_d = \boldsymbol{\tau} \quad (1)$$

where $\mathbf{M}(\mathbf{q})$ is the inertia matrix, $\mathbf{C}(\mathbf{q}, \dot{\mathbf{q}})$ is the Coriolis/centrifugal matrix, $\mathbf{G}(\mathbf{q})$ stands for the gravity vector, $\mathbf{Fr}(\mathbf{q}, \dot{\mathbf{q}})$ represents the friction vector, and $\boldsymbol{\tau}_d$ stands for the lumped unknown disturbance, while $\boldsymbol{\tau}$ is the control torque vector.

To effectively apply TDC, the above dynamic equation is reexpressed as

$$\overline{\mathbf{M}} \ddot{\mathbf{q}} + \mathbf{h} = \boldsymbol{\tau} \quad (2)$$

where $\overline{\mathbf{M}}$ is a constant control parameter to be tuned by simulations afterwards, while \mathbf{h} stands for the complicated lumped remaining dynamics of the robot manipulators except $\overline{\mathbf{M}} \ddot{\mathbf{q}}$. The term \mathbf{h} is defined as

$$\mathbf{h} = (\mathbf{M} - \overline{\mathbf{M}}) \mathbf{M}(\mathbf{q}) \ddot{\mathbf{q}} + \mathbf{C}(\mathbf{q}, \dot{\mathbf{q}}) \dot{\mathbf{q}} + \mathbf{G}(\mathbf{q}) + \mathbf{Fr}(\mathbf{q}, \dot{\mathbf{q}}) + \boldsymbol{\tau}_d \quad (3)$$

It can be observed clearly from (3) that the element \mathbf{h} is extremely complicated, which contains strong nonlinearities and high couplings and unknown time-varying disturbances. Therefore, it can be very difficult to obtain \mathbf{h} using traditional method. Then, the goal of this paper can be described as follows: given a reference trajectory \mathbf{q}_d , design a model-free and simple control scheme for the robot manipulators to track \mathbf{q}_d as precisely as possible.

2.2. TDC Scheme with Linear Error Dynamics. As discussed above, the element \mathbf{h} can be very difficult or time-consuming to obtain with conventional methods. Conventional methods, like adaptive techniques and fuzzy logic methods and other intelligent schemes, usually need detailed system model or lots of parameters to get \mathbf{h} . However, the detailed system model is usually quite difficult to get in complicated real situations. Also, too many estimation parameters will make the algorithm not easy to use. What we need is a simple and straightforward scheme to obtain \mathbf{h} ; meanwhile, the validity

and estimation accuracy should also be guaranteed. To realize the above requirement, we use TDC scheme in this paper. The core element of TDC scheme is the so-called time delay estimation (TDE), which uses time-delayed values of the system states to estimate the remaining dynamics \mathbf{h} . For TDE, it can be described by the following equation [14–20]:

$$\hat{\mathbf{h}}(t) \cong \mathbf{h}(t-L) = \boldsymbol{\tau}(t-L) - \overline{\mathbf{M}}\ddot{\mathbf{q}}(t-L) \quad (4)$$

where L is the delayed time and usually selected as one or several sampling periods. It can be observed from (4) that no system model information is used and therefore a fascinating model-free feature can be effectively obtained.

Define the control error as

$$\mathbf{e} = \mathbf{q}_d - \mathbf{q} \quad (5)$$

Then, the classical TDC scheme with linear error dynamics can be given as [14–20]

$$\begin{aligned} \boldsymbol{\tau} &= \overline{\mathbf{M}}(\ddot{\mathbf{q}}_d + \mathbf{k}_p \mathbf{e} + \mathbf{k}_d \dot{\mathbf{e}}) + \hat{\mathbf{h}}(t) \\ &= \underbrace{\overline{\mathbf{M}}(\ddot{\mathbf{q}}_d + \mathbf{k}_p \mathbf{e} + \mathbf{k}_d \dot{\mathbf{e}})}_{\text{Injected dynamics}} + \underbrace{\boldsymbol{\tau}(t-L) - \overline{\mathbf{M}}\ddot{\mathbf{q}}(t-L)}_{\text{TDE}} \end{aligned} \quad (6)$$

where \mathbf{k}_p and \mathbf{k}_d are positive constant control parameters.

As shown in (6), therefore, there are mainly two parts in the classical TDC scheme: the TDE part and the injected dynamics part. The former is used to estimate the lumped remaining system dynamics and bring in an attractive model-free nature; meanwhile, the latter is utilized to ensure the desired dynamic performance and high control accuracy. Due to the application of time-delayed system states in TDE scheme as shown in (4), the estimation error is usually unavoidable especially when system experiences abrupt changes. Therefore, the injected dynamics should be robust enough to obtain good control accuracy and fast dynamics response, which, however, can be an extremely challenging job for the above linear error dynamics. Since the upper boundary information is usually unknown, thus sufficiently large control gains \mathbf{k}_p and \mathbf{k}_d are usually used to ensure satisfactory control performance, which in turn may lead to obvious increasing of the noise effect and control performance deterioration.

2.3. TDC Scheme Design with ANTSM Dynamics. To effectively settle the above-mentioned issues and ensure high control performance for the robot manipulators, we design a new TDC scheme with ANTSM dynamics.

The NTSM manifold is designed as

$$\mathbf{s} = \mathbf{e} + \mathbf{k} \text{sig}(\dot{\mathbf{e}})^a \quad (7)$$

where \mathbf{k} and \mathbf{a} are positive constant control parameters and $1 < a_i < 2, i = 1 \sim n$. The notation $\text{sig}(\mathbf{e})^a$ is defined as $\text{sig}(\mathbf{e})^a = [|\dot{e}_1|^{a_1} \text{sgn}(\dot{e}_1), \dots, |\dot{e}_n|^{a_n} \text{sgn}(\dot{e}_n)]^T$, with the sign function given as

$$\text{sgn}(e_i) = \begin{cases} 1, & \text{if } e_i > 0 \\ 0, & \text{if } e_i = 0 \\ -1, & \text{if } e_i < 0 \end{cases} \quad (8)$$

To ensure both high control accuracy and effective chattering suppression simultaneously, we use the following combined adaptive reaching law as

$$\dot{\mathbf{s}} = -\boldsymbol{\rho}_1 \mathbf{s} - \boldsymbol{\rho}_2 \text{sig}(\mathbf{s})^\beta - \widehat{\mathbf{K}}(t) \text{sgn}(\mathbf{s}) \quad (9)$$

where $\boldsymbol{\rho}_1, \boldsymbol{\rho}_2, \beta$ are positive constant control parameters and $0 < \beta < 1$. Meanwhile, the adaptive control gain $\widehat{\mathbf{K}}(t)$ is updated using the following adaptive law:

$$\dot{\widehat{K}}_i(t) = \begin{cases} \eta_i, & \widehat{K}_i \leq K_{\min,i} \\ \eta_i \text{sgn}(|s_i| - \Delta_i), & K_{\min,i} < \widehat{K}_i < K_{\max,i} \\ -\eta_i, & \widehat{K}_i \geq K_{\max,i} \end{cases} \quad (10)$$

where η_i, Δ_i are constant parameters and $K_{\min,i}$ and $K_{\max,i}$ are the predescribed minimum and maximum values of the adaptive gain $\widehat{K}_i(t)$. As shown in (10), the parameter η_i is used to determine the adaptive speed, while Δ_i is used to decide when $\widehat{K}_i(t)$ increases or decreases. It should be noted that the adaptive gain $\widehat{\mathbf{K}}(t)$ is naturally bounded as $K_{\min,i} \leq \widehat{K}_i \leq K_{\max,i}$ using the proposed adaptive law (10).

Different from the existing TDC schemes [14–27], our proposed TDC scheme uses a combined reaching law to enhance the control performance under time-varying uncertainties. Taking (9) and (10) for further analysis, we can see that the combined reaching law has two elements, i.e., a well-known fast-TSM-type reaching law and a constant speed reaching law with adaptive gain. The former is used to ensure high control accuracy and fast dynamic response in the whole control process; meanwhile, the latter is mainly used to provide extra robustness against unknown lumped disturbance. When the control performance is relatively satisfactory, the fast-TSM-type reaching law will dominate the whole combined reaching law (9) and bring in continuous high control performance. On the other hand, when the control errors tend to increase, the adaptive gain $\widehat{\mathbf{K}}(t)$ will increase rapidly and then the latter part will take over the combined reaching law. Afterwards, the control errors will be strongly suppressed by the extra robustness provided by the part $\widehat{\mathbf{K}}(t) \text{sgn}(\mathbf{s})$. Thanks to the novel combined reaching law and proposed adaptive law, high control accuracy and fast dynamic response and effective suppression of the chatter can be obtained simultaneously. Moreover, the utilization of above adaptive law can also effectively suppress the potential chatters by rapidly reducing the gain $\widehat{\mathbf{K}}(t)$ when the control performance is satisfactory. Above claims will be demonstrated in the simulation studies given afterwards.

Finally, combining the designed NTSM manifold (7) and proposed combined reaching law (9)–(10) with the TDC scheme (6), we have

$$\begin{aligned} \boldsymbol{\tau} &= \underbrace{\overline{\mathbf{M}}(\ddot{\mathbf{q}}_d + \mathbf{a}^{-1} \mathbf{k}^{-1} \text{sig}(\dot{\mathbf{e}})^{2-a})}_{\text{NTSM error dynamics}} \\ &\quad + \underbrace{\overline{\mathbf{M}}(\boldsymbol{\rho}_1 \mathbf{s} + \boldsymbol{\rho}_2 \text{sig}(\mathbf{s})^\beta + \widehat{\mathbf{K}}(t) \text{sgn}(\mathbf{s}))}_{\text{Combined reaching law}} \\ &\quad + \underbrace{\boldsymbol{\tau}(t-L) - \overline{\mathbf{M}}\ddot{\mathbf{q}}(t-L)}_{\text{TDE}} \end{aligned} \quad (11)$$

As depicted in (11), our newly proposed method has three parts: the TDE part applied to ensure the model-free nature and bring in simple control scheme, the combined reaching law part utilized to ensure high control accuracy and fast dynamic response and good robustness in the reaching phase, and the NTSM error dynamics part used to obtain fast convergence and high control accuracy in the sliding mode phase. The working mechanism and advantages of the proposed combined reaching law part have been carefully discussed earlier.

Remark 1. To ensure good control performance with our newly proposed TDC scheme, proper control parameters are required. It should be noted that the delayed time L is usually selected as one or several periods. Then, the following parameter tuning procedures can be utilized [44]:

- (1) Set $\mathbf{k}=\mathbf{a}=\boldsymbol{\rho}_1=\boldsymbol{\rho}_2=1_n$, $\eta = \widehat{\mathbf{K}}(t=0) = 0$; then tune $\overline{\mathbf{M}}$ by increasing it from small one to large one until the control performance tends to degrade.
- (2) Set $\mathbf{a}=\boldsymbol{\rho}_1=\boldsymbol{\rho}_2=1_n$, $\eta = \widehat{\mathbf{K}}(t=0) = 0$; then tune \mathbf{k} by reducing it from large one to small one and check the control performance; tune \mathbf{a} by increasing it from 1_n to 2 and check the control performance.
- (3) Set $\eta = \widehat{\mathbf{K}}(t=0) = 0$; tune $\boldsymbol{\rho}_1$ and $\boldsymbol{\rho}_2$ by increasing them from small ones to large ones and check the control performance.
- (4) Set $\eta=0$, $\widehat{\mathbf{K}}(t=0) = \mathbf{K}_{\max}$; tune K_{\max} by increasing it from small one to large one until the system tends to chatter.
- (5) Set $\eta=0$, $\widehat{\mathbf{K}}(t=0) = \mathbf{K}_{\min}$; tune K_{\min} by decreasing it from K_{\max} to small one and check the control performance.
- (6) Set $\widehat{\mathbf{K}}(t=0) = \mathbf{K}_{\min}$; tune η by increasing it from small one to large one and check the control performance; Δ can be tuned using the same procedure.

3. Stability Analysis

In this section, the stability of the closed-loop control system is analyzed. Before giving the analysis results, the following lemma will be necessary.

Lemma 2 (see [45]). *For a system $\dot{x} = f(x, y)$, suppose inequality (12) holds for a continuous function $V(x)$ with $\rho > 0$, $0 < \beta < 1$, $0 < \eta < \infty$:*

$$\dot{V}(x) \leq -\rho V^\beta(x) + \eta \quad (12)$$

Then, the system $\dot{x} = f(x, y)$ is defined as practical finite time stable (PFS), and the system trajectory will be enforced into the following field (13) using finite time T as (14):

$$\lim_{\varphi \rightarrow \varphi_0} x \in \left(V^\beta(x) \leq \frac{\eta}{(1-\varphi)\rho} \right) \quad (13)$$

$$T \leq \frac{V^{1-\beta}(x_0)}{\rho\varphi_0(1-\beta)} \quad (14)$$

where $0 < \varphi_0 < 1$ and $V(x_0)$ stands for the initial value of $V(x)$.

Substituting the proposed control (11) into the system dynamics (2), we have

$$\begin{aligned} \ddot{\mathbf{e}} + \mathbf{a}^{-1}\mathbf{k}^{-1}\mathbf{sig}(\dot{\mathbf{e}})^{2-a} + \boldsymbol{\rho}_1\mathbf{s} + \boldsymbol{\rho}_2\mathbf{sig}(\mathbf{s})^\beta + \widehat{\mathbf{K}}(t)\mathbf{sgn}(\mathbf{s}) \\ = \boldsymbol{\delta}(t) \end{aligned} \quad (15)$$

where the element $\boldsymbol{\delta}(t)$ is the so-called TDE error and is given as

$$\boldsymbol{\delta}(t) = -\overline{\mathbf{M}}^{-1}(\widehat{\mathbf{h}} - \mathbf{h}) \quad (16)$$

It can be seen from (16) that $\boldsymbol{\delta}(t)$ is mainly caused by the applications of time-delayed values of system states and is usually unavoidable. On the other hand, $\boldsymbol{\delta}(t)$ has been broadly proven to be bounded for lots of systems including robot manipulators [17].

Define $\widetilde{K}_i = K_i - \widehat{K}_i$, where K_i is a positive constant parameter. Meanwhile, bring in a new nonnegative variable $\lambda_i = k_i a_i |\dot{e}_i|^{a_i-1} \geq 0$. For simplicity, we will take the i -DOF to analyze in what follows. Then, following Lyapunov function is chosen as

$$V_i = \frac{1}{2}s_i^2 + \frac{\lambda_i}{2}\widetilde{K}_i^2 \quad (17)$$

Differentiating (17) along time, we have

$$\begin{aligned} \dot{V}_i &= s_i\dot{s}_i + \lambda_i\widetilde{K}_i\dot{\widetilde{K}}_i = s_i(\dot{e}_i + k_i a_i |\dot{e}_i|^{a_i-1}\dot{e}_i) - \lambda_i\widetilde{K}_i\dot{\widetilde{K}}_i \\ &= s_i\lambda_i(\delta_i - \rho_{1i}s_i - \rho_{2i}\mathbf{sig}(s_i)^\beta - \widehat{K}_i\mathbf{sgn}(s_i)) \\ &\quad - \lambda_i\widetilde{K}_i\dot{\widetilde{K}}_i \\ &= -s_i(\overline{\rho}_{1i}s_i + \overline{\rho}_{2i}\mathbf{sig}(s_i)^\beta) - \lambda_i\widetilde{K}_i|s_i| + \lambda_i s_i \delta_i \\ &\quad - \lambda_i\widetilde{K}_i\dot{\widetilde{K}}_i \end{aligned} \quad (18)$$

where $\overline{\rho}_{1i} = \lambda_i \rho_{1i}$, $\overline{\rho}_{2i} = \lambda_i \rho_{2i}$.

Considering the adaptive law (10), (18) can be further given as

$$\begin{aligned} \dot{V}_i &\leq -s_i(\overline{\rho}_{1i}s_i + \overline{\rho}_{2i}\mathbf{sig}(s_i)^\beta) - \lambda_i|s_i|(\widehat{K}_i - |\delta_i|) \\ &\quad + \eta_i\lambda_i|\widetilde{K}_i| \end{aligned} \quad (19)$$

Since the TDE error $\boldsymbol{\delta}(t)$ is usually quite small; therefore, it can be easy to select a proper large $K_{\min,i}$ such that $K_{\min,i} \geq |\delta_i|$ holds for $t \geq 0$. Meanwhile, the element $|\widetilde{K}_i|$ is obvious bounded considering the boundedness of $\widehat{\mathbf{K}}(t)$.

Then, (19) can be given as

$$\dot{V}_i \leq -s_i(\overline{\rho}_{1i}s_i + \overline{\rho}_{2i}\mathbf{sig}(s_i)^\beta) + \eta_i\lambda_i|\widetilde{K}_i| \quad (20)$$

Equation (20) can be further reexpressed into the following two inequalities:

$$\dot{V}_i \leq -\overline{\rho}_{2i}|s_i|^{\beta+1} + \eta_i\lambda_i|\widetilde{K}_i| \quad (21)$$

$$\dot{V}_i \leq -\overline{\rho}_{1i}s_i^2 + \eta_i\lambda_i|\widetilde{K}_i| \quad (22)$$

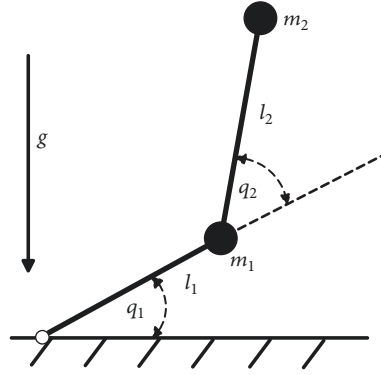


FIGURE 1: 2-DOFs robot manipulators.

For (21), it can be rewritten into the following form:

$$\begin{aligned} \dot{V}_i &\leq -2^{(\beta+1)/2} \bar{\rho}_{2i} \left(\frac{1}{2} s_i^2 \right)^{(\beta+1)/2} \\ &\quad - 2^{(\beta+1)/2} \bar{\rho}_{2i} \left(\frac{1}{2} \tilde{K}_i^2 \right)^{(\beta+1)/2} \\ &\quad + 2^{(\beta+1)/2} \bar{\rho}_{2i} \left(\frac{1}{2} \tilde{K}_i^2 \right)^{(\beta+1)/2} + \eta_i \lambda_i |\tilde{K}_i| \\ &= -\theta_{1i} \left(\left(\frac{1}{2} s_i^2 \right)^{(\beta+1)/2} + \left(\frac{1}{2} \tilde{K}_i^2 \right)^{(\beta+1)/2} \right) + \omega_{1i} \end{aligned} \quad (23)$$

where $\theta_{1i} = 2^{(\beta+1)/2} \bar{\rho}_{2i}$, $\omega_{1i} = 2^{(\beta+1)/2} \bar{\rho}_{2i} \left((1/2) \tilde{K}_i^2 \right)^{(\beta+1)/2} + \eta_i \lambda_i |\tilde{K}_i|$.

Considering a well-known inequality $(|x_1| + |x_2|)^y \leq |x_1|^y + |x_2|^y$, x_1, x_2 are real numbers and $0 < y \leq 1$; then the above inequality (23) can be further written as

$$\dot{V}_i \leq -\theta_{1i} V_i^{(\beta+1)/2} + \omega_{1i} \quad (24)$$

Therefore, the system trajectories will be enforced to the following fields within finite time based on Lemma 2:

$$|s_i| \leq \left(\frac{\omega_{1i}}{(1 - \varphi_i) \theta_{1i}} \right) \quad (25)$$

Using the same analysis method for (22), similar results can be obtained as

$$|s_i| \leq \left(\frac{\omega_{2i}}{(1 - \varphi_i) \theta_{2i}} \right) \quad (26)$$

where $\theta_{1i} = 2 \bar{\rho}_{1i}$, $\omega_{1i} = \bar{\rho}_{1i} \tilde{K}_i^2 + \eta_i \lambda_i |\tilde{K}_i|$.

Thus, the system trajectories will be enforced into the following fields in finite time:

$$\Omega_i = \min \left\{ \left(\frac{\omega_{1i}}{(1 - \varphi_i) \theta_{1i}} \right), \left(\frac{\omega_{2i}}{(1 - \varphi_i) \theta_{2i}} \right) \right\} \quad (27)$$

It should be noted that $\lambda_i = 0$; i.e., $\dot{e}_i = 0$ may hinder the reachability of NTSM manifold (7), which, however, will be

analyzed in what follows. Substituting $\dot{e}_i = 0$ and $s_i \neq 0$ into (15), we have

$$\ddot{e}_i = \delta_i(t) - \rho_{1i} s_i - \rho_{2i} \text{sig}(s_i)^\beta - \tilde{K}_i \text{sgn}(s_i) \quad (28)$$

It is obvious that $\ddot{e}_i = 0$ will not be always satisfied with $\dot{e}_i = 0$ and $s_i \neq 0$. Therefore, $\lambda_i = 0$ will not hinder the reachability of NTSM manifold (7).

Substituting (27) into (7), we have

$$s_i = e_i + k_i \text{sig}(\dot{e}_i)^{a_i}, \quad |s_i| \leq \Omega_i \quad (29)$$

The above equation can be further restructured as

$$e_i + (k_i - s_i \text{sig}(\dot{e}_i)^{-a_i}) \text{sig}(\dot{e}_i)^{a_i} = 0 \quad (30)$$

Equation (30) will still be NTSM manifold form as (7) under the condition that $(k_i - s_i \text{sig}(\dot{e}_i)^{-a_i}) > 0$ holds; therefore, \dot{e}_i will converge to the following field within finite time:

$$|\dot{e}_i| \leq |s_i k_i^{-1}|^{1/a_i} \leq |\Omega_i k_i^{-1}|^{1/a_i} = \Omega_{\dot{e}_i} \quad (31)$$

Substituting (31) into (29), we have

$$|e_i| = |s_i - k_i \text{sig}(\dot{e}_i)^{a_i}| \leq |s_i| + |k_i \text{sig}(\dot{e}_i)^{a_i}| = 2\Omega_i \quad (32)$$

Thus, the system trajectories will be enforced into the field (27), (31), and (32) within finite time. Then, the stability of the closed-loop control system is proved.

4. Simulation Studies

To demonstrate the effectiveness and advantages of our newly proposed TDC scheme with ANTSM dynamics, comparative simulations were conducted using 2-DOFs (degree of freedoms) robot manipulators as indicated in Figure 1.

4.1. Simulation Setup. The system dynamics used in the following simulations are directly taken from [15] with different design of lumped uncertainties for both joints as $\tau_d = \sin(\pi t)$ N•m. The detailed system dynamics are [17]

$$\mathbf{M}(\mathbf{q}) = \begin{bmatrix} M_{11} & M_{12} \\ M_{21} & M_{22} \end{bmatrix},$$

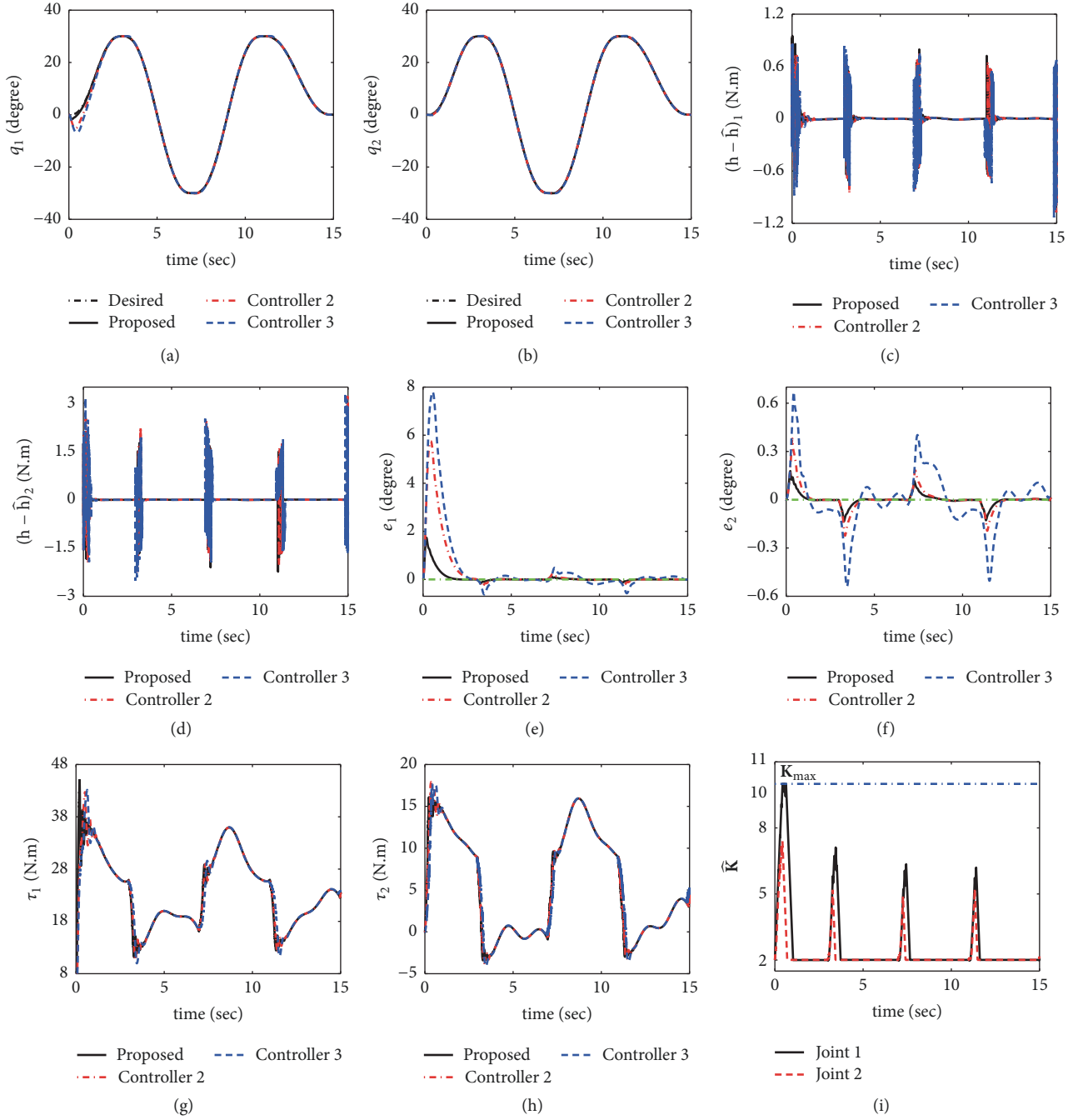


FIGURE 2: Simulation results of Case one: (a) and (b) are trajectory tracking performance for joints 1 and 2, respectively; (c) and (d) are estimation error $\mathbf{h} - \hat{\mathbf{h}}$ for joints 1 and 2, respectively; (e) and (f) are tracking errors for joints 1 and 2, respectively; (g) and (h) are control efforts for joints 1 and 2, respectively; (i) is the adaptive gain $\hat{\mathbf{K}}$ for joints 1 and 2, respectively.

$$\begin{aligned}
 M_{11} &= l_2^2 m_2 + 2l_1 l_2 m_2 \cos(q_2) + l_1^2 (m_1 + m_2) \\
 M_{12} &= M_{21} = l_2^2 m_2 + l_1 l_2 m_2 \cos(q_2), \\
 M_{22} &= l_2^2 m_2
 \end{aligned}
 \quad
 \mathbf{G}(\mathbf{q}) = \begin{bmatrix} -l_1 l_2 m_2 \sin(q_2) \dot{q}_2^2 - 2l_1 l_2 m_2 \sin(q_2) \dot{q}_1 \dot{q}_2 \\ l_1 l_2 m_2 \sin(q_2) \dot{q}_2^2 \end{bmatrix} \quad (34)$$

$$\mathbf{C}(\mathbf{q}, \dot{\mathbf{q}}) \dot{\mathbf{q}} = \begin{bmatrix} l_2 m_2 g \cos(q_1 + q_2) + (m_1 + m_2) l_1 g \cos(q_1) \\ l_2 m_2 g \cos(q_1 + q_2) \end{bmatrix} \quad (35)$$

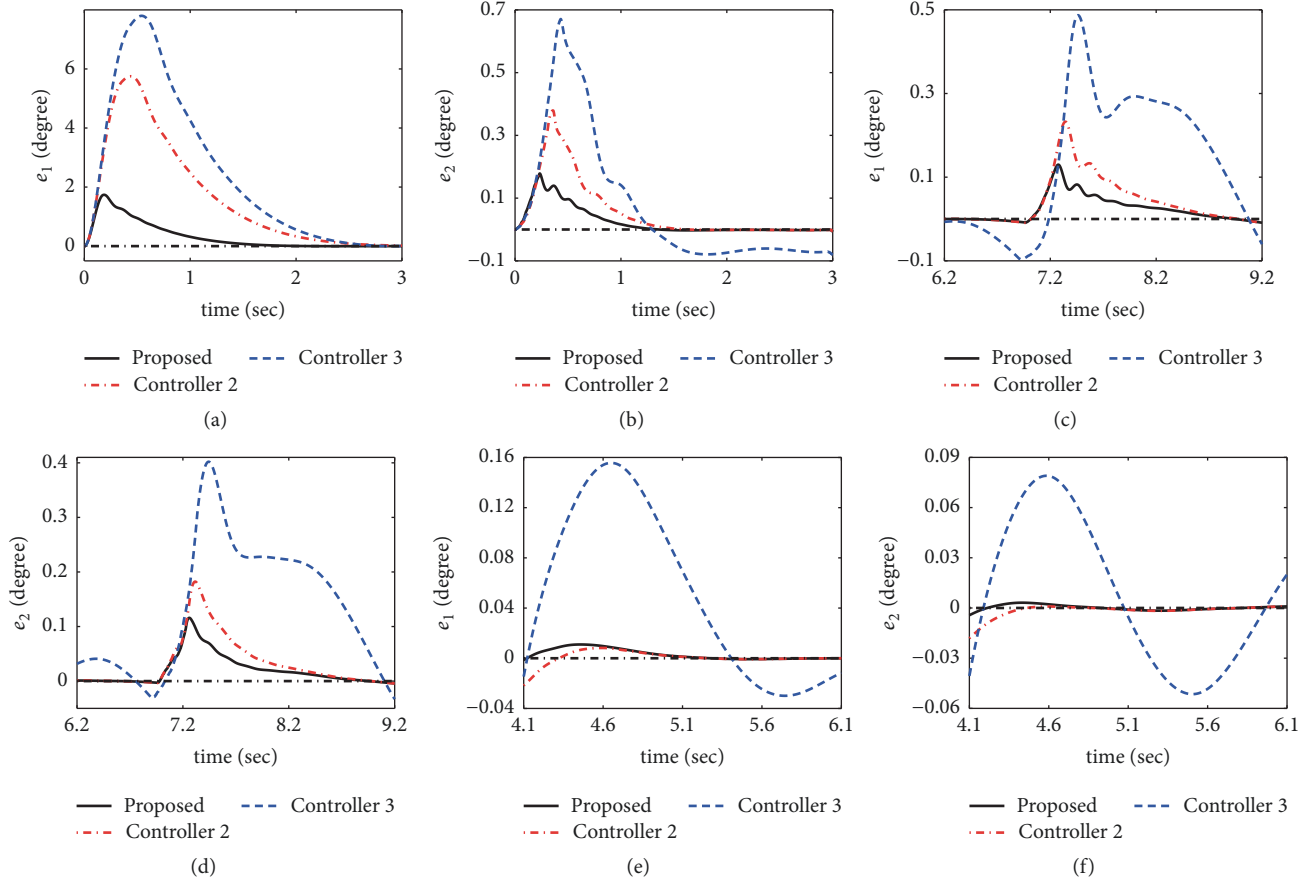


FIGURE 3: Simulation results of Case one: (a) and (b) are control errors within initial phase $t \in [1, 3]$ sec for joints 1 and 2, respectively; (c) and (d) are control errors within peak phase $t \in [6.2, 9.2]$ sec for joints 1 and 2, respectively; (e) and (f) are control errors within steady phase $t \in [4.1, 6.1]$ sec for joints 1 and 2, respectively.

$$\mathbf{Fr}(\mathbf{q}, \dot{\mathbf{q}}) = \begin{bmatrix} F_{v1}\dot{q}_1 + F_{c1}\text{sgn}(\dot{q}_1) \\ F_{v2}\dot{q}_2 + F_{c2}\text{sgn}(\dot{q}_2) \end{bmatrix} \quad (36)$$

where l_i , m_i , g , F_{vi} , F_{ci} stand for the link length, mass, local acceleration, viscous, and Coulomb friction for the i -DOF, respectively. The dynamical parameters are $l_1 = 1$ m, $l_2 = 0.8$ m, $m_1 = m_2 = 1$ kg, $F_{v1} = F_{v2} = 5$ N·m·s/rad, $F_{c1} = F_{c2} = 5$ N·m, and $g = 9.8$ m/s².

Three TDC schemes are taken for comparisons. The first one is our newly proposed TDC with ANTSM (11), (10). The other two, referred to as Controller 2 and Controller 3, are taken from [17, 42, 43] as

$$\begin{aligned} \boldsymbol{\tau} = & \underbrace{\overline{\mathbf{M}}(\ddot{\mathbf{q}}_d + \mathbf{a}^{-1}\mathbf{k}^{-1}\text{sig}(\dot{\mathbf{e}})^{2-a})}_{\text{NTSM error dynamics}} \\ & + \underbrace{\overline{\mathbf{M}}(\rho_1\mathbf{s} + \rho_2\text{sat}(\text{sig}(\mathbf{s})^\beta/\varphi^\beta))}_{\text{reaching law}} \\ & + \underbrace{\boldsymbol{\tau}(t-L) - \overline{\mathbf{M}}\ddot{\mathbf{q}}(t-L)}_{\text{TDE}} \end{aligned} \quad (37)$$

$$\begin{aligned} \boldsymbol{\tau} = & \underbrace{\overline{\mathbf{M}}(\ddot{\mathbf{q}}_d + \mathbf{a}^{-1}\mathbf{k}^{-1}\text{sig}(\dot{\mathbf{e}})^{2-a} + \rho_2\text{sat}(\mathbf{s}/\varphi))}_{\text{NTSM error dynamics}} \\ & + \underbrace{\boldsymbol{\tau}(t-L) - \overline{\mathbf{M}}\ddot{\mathbf{q}}(t-L)}_{\text{TDE}} \end{aligned} \quad (38)$$

with NTSM manifold designed as (7). The parameter φ stands for the boundary layer.

To make the comparison fair and also suppress the potential chatters, our newly proposed TDC scheme with ANTSM dynamics is also modified as

$$\begin{aligned} \boldsymbol{\tau} = & \underbrace{\overline{\mathbf{M}}(\ddot{\mathbf{q}}_d + \mathbf{a}^{-1}\mathbf{k}^{-1}\text{sig}(\dot{\mathbf{e}})^{2-a})}_{\text{NTSM error dynamics}} \\ & + \underbrace{\overline{\mathbf{M}}(\rho_1\mathbf{s} + \rho_2\text{sat}(\text{sig}(\mathbf{s})^\beta/\varphi^\beta) + \widehat{\mathbf{K}}(t)\text{sat}(\mathbf{s}/\varphi))}_{\text{Combined reaching law}} \\ & + \underbrace{\boldsymbol{\tau}(t-L) - \overline{\mathbf{M}}\ddot{\mathbf{q}}(t-L)}_{\text{TDE}} \end{aligned} \quad (39)$$

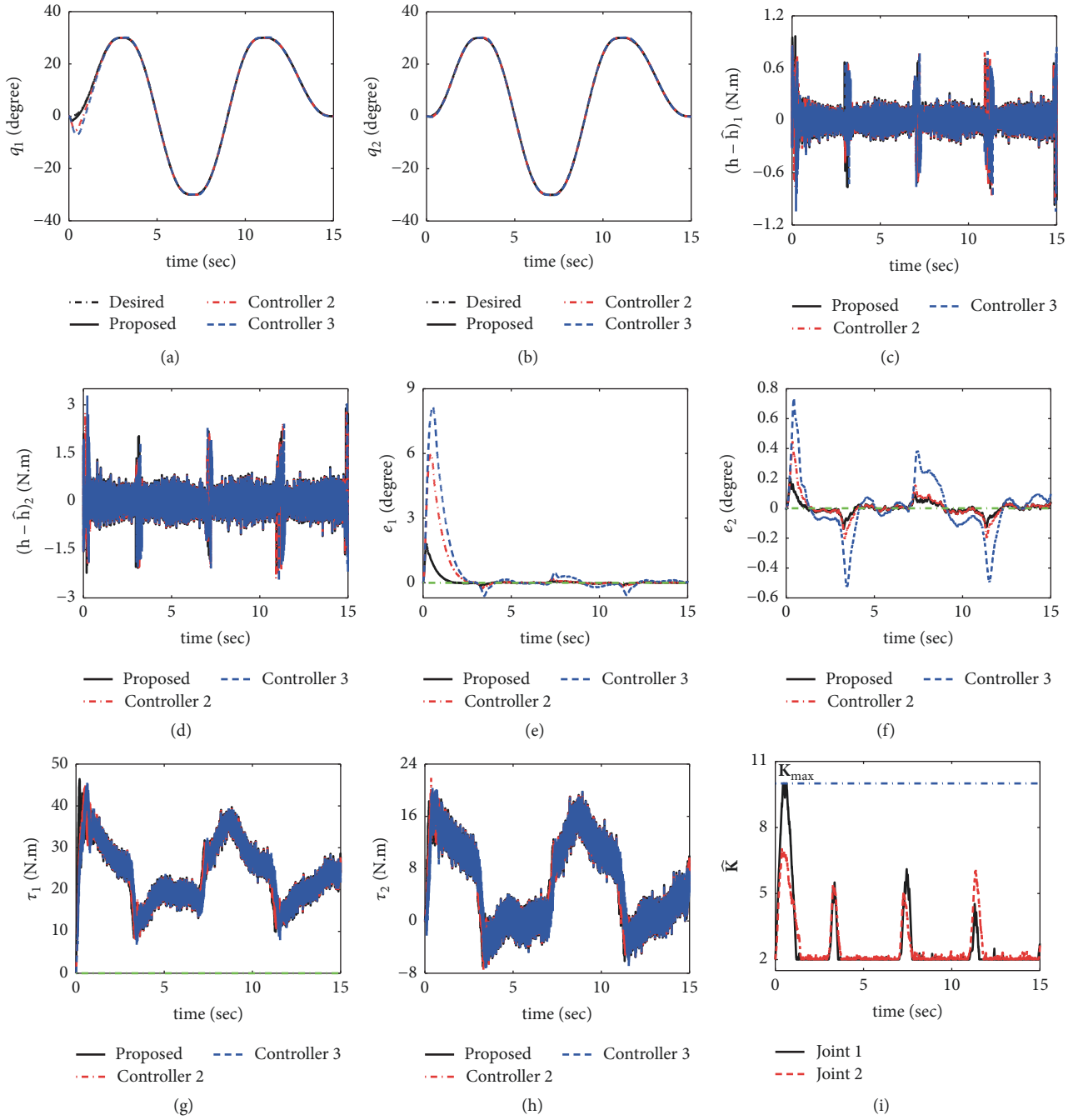


FIGURE 4: Simulation results of Case two: (a) and (b) are trajectory tracking performance for joints 1 and 2, respectively; (c) and (d) are estimation error $\mathbf{h} - \hat{\mathbf{h}}$ for joints 1 and 2, respectively; (e) and (f) are tracking errors for joints 1 and 2, respectively; (g) and (h) are control efforts for joints 1 and 2, respectively; (i) is the adaptive gain $\hat{\mathbf{K}}$ for joints 1 and 2, respectively.

4.2. Simulation Results. Three cases were simulated for comprehensive demonstration of the newly proposed control scheme. First, the robot manipulator is commanded to track a smooth reference trajectory with no consideration of measurement noise. Second, the measurement noise is taken into consideration based on Case one. Third, the robot manipulator is commanded to track a combined triangular

wave signal. The control parameters for our proposed method are selected as $\mathbf{k} = \text{diag}(1, 1)$, $\mathbf{a} = \text{diag}(1.2, 1.2)$, $\boldsymbol{\rho}_1 = \boldsymbol{\rho}_2 = \text{diag}(2, 2)$, $\beta = 0.5$, $\boldsymbol{\eta} = \text{diag}(20, 20)$, $\boldsymbol{\Delta} = 0.001 \times \text{diag}(2, 2)$, $\mathbf{K}_{\min} = \text{diag}(2, 2)$, $\mathbf{K}_{\max} = \text{diag}(10, 10)$, $\varphi = 0.05$, $\bar{\mathbf{M}} = 0.01 \times \text{diag}(5, 5)$, and $L = 1\text{ms}$. Meanwhile, the initial value of $\hat{\mathbf{K}}(t)$ is set to \mathbf{K}_{\min} , and the sampling period of the simulation is set to 1ms. For comparison fairness, the control

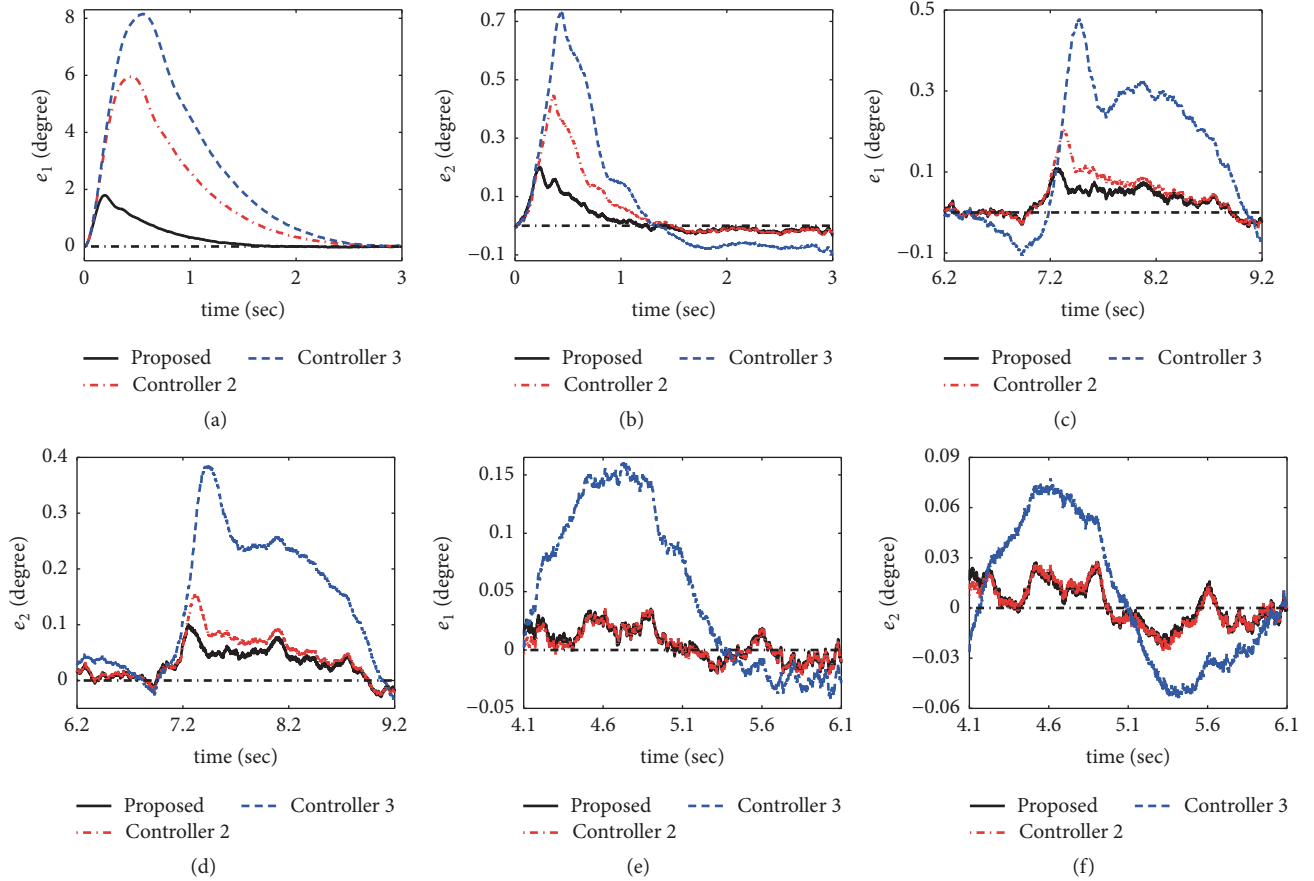


FIGURE 5: Simulation results of Case two: (a) and (b) are control errors within initial phase $t \in [1, 3]$ sec for joints 1 and 2, respectively; (c) and (d) are control errors within peak phase $t \in [6.2, 9.2]$ sec for joints 1 and 2, respectively; (e) and (f) are control errors within steady phase $t \in [4.1, 6.1]$ sec for joints 1 and 2, respectively.

parameters for the other two TDC schemes (37) and (38) are selected exactly the same as ours. Furthermore, a time-varying lumped disturbance $\tau_d = \sin(\pi t)$ N•m is added to both joints in the simulation to demonstrate the robustness of our proposed TDC scheme.

4.2.1. Case One. In this case, the robot manipulator is commanded to track a smooth reference trajectory, which is obtained through fifth-order polynomial method using the initial and terminate points listed in Table 1. Finally, the simulation results are given in Figures 2 and 3.

As shown in the simulation results in Figures 2 and 3, all three control schemes can provide good reference trajectory tracking control performance under time-varying lumped disturbance τ_d . High control accuracy and fast convergence have been clearly observed as shown in Figures 2(e), 2(f), and 3(a)–3(f). The above results strongly demonstrate the effectiveness of TDC scheme and NTSM error dynamics. Meanwhile, our proposed TDC scheme with a novel ANTSM dynamics can still ensure the best comprehensive control performance as shown in Figures 2(e), 2(f), and 3(a)–3(f). Faster dynamical response and higher control accuracy can be clearly seen from these simulation results. For further

analysis, we take Figure 2(i) to analyze. It can be seen that the adaptive gain $\widehat{K}(t)$ will rapidly increase when the control performance tend to degrade, which in turn will bring in extra control efforts and robustness. Then, high control accuracy and strong robustness can be effectively obtained. Meanwhile, $\widehat{K}(t)$ will rapidly decrease when the control performance is relatively satisfactory. Therefore, relative smaller control efforts will be generated. Thanks to this adaptive mechanism, high comprehensive control performance and effective suppression of the chattering and noise effect can be ensured simultaneously.

4.2.2. Case Two. In this case, the measurement noise is taken into consideration, which is simulated using a band-limited white noise module with noise power of 10^{-8} and sampling time of 1 ms. The reference trajectory is selected the same as Case one. The obtained simulation results are given Figures 4 and 5. As indicated in Figures 4 and 5, the introduction of measurement noise has led to clear noisy performance of control effort but bounded without any noticeable chattering. Still, our proposed method can provide the best comprehensive control performance among all three TDC schemes as shown in Figures 4(e), 4(f), and 5. Higher

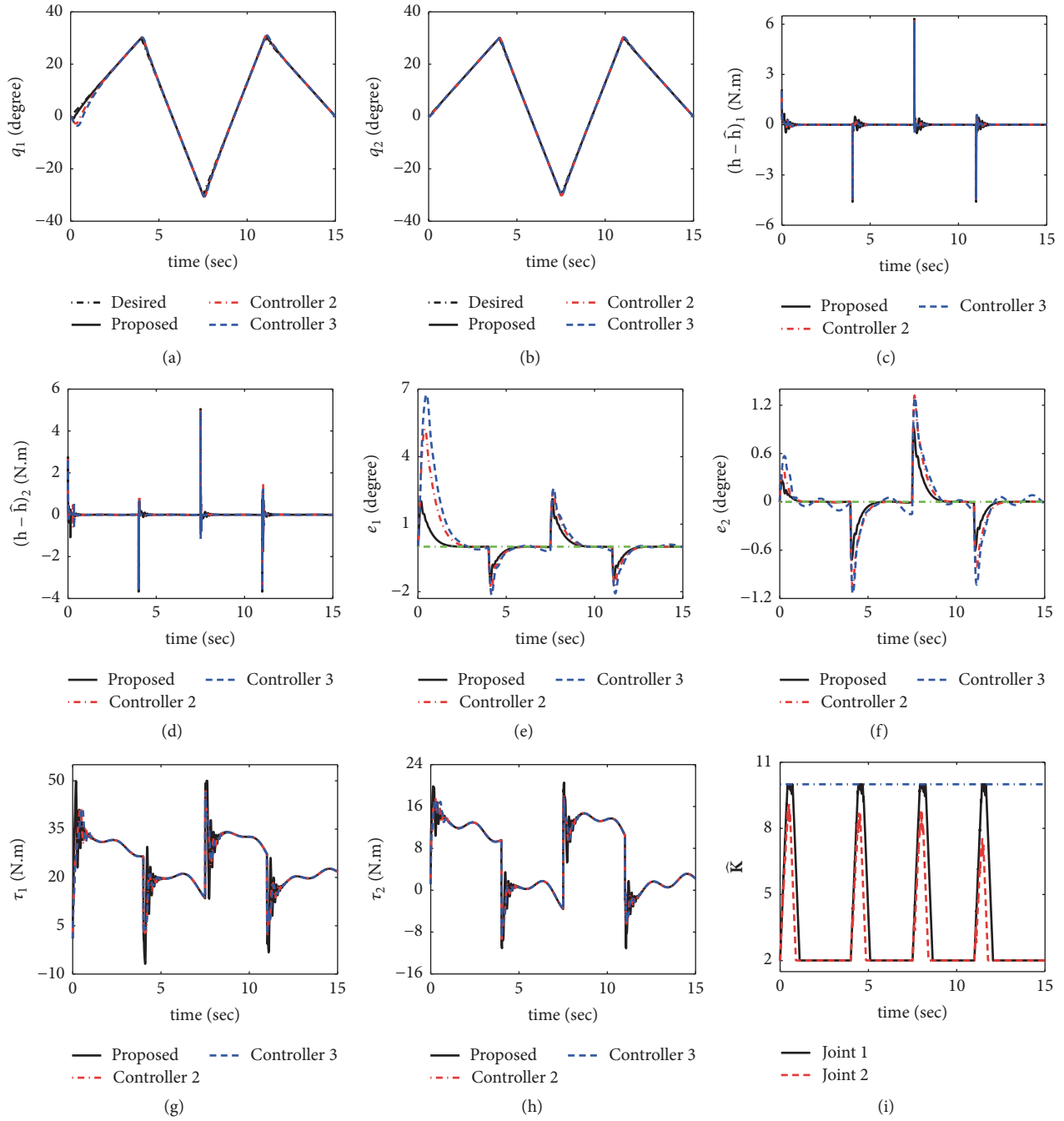


FIGURE 6: Simulation results of Case three: (a) and (b) are trajectory tracking performance for joints 1 and 2, respectively; (c) and (d) are estimation error $\mathbf{h} - \hat{\mathbf{h}}$ for joints 1 and 2, respectively; (e) and (f) are tracking errors for joints 1 and 2, respectively; (g) and (h) are control efforts for joints 1 and 2, respectively; (i) is the adaptive gain $\hat{\mathbf{K}}$ for joints 1 and 2, respectively.

control accuracy, faster convergence, and stronger robustness have been clearly observed with our newly proposed method under measurement noise.

4.2.3. Case Three. to further verify the effectiveness of our proposed method, a combined triangular wave signal with two different speeds is sent to the robot manipulator as shown in Figures 6(a) and 6(b). Corresponding simulation results

are given in Figures 6 and 7. As shown in Figures 6 and 7, satisfactory control performance can still be ensured with all three control schemes under this reference trajectory. On the other hand, our proposed method can still provide the best control performance as indicated in Figures 6(e), 6(f), and 7. Furthermore, taking Figures 6(h) and 6(i) to analyze, we can see that when the reference trajectory changes suddenly, the adaptive mechanism will generate large extra control

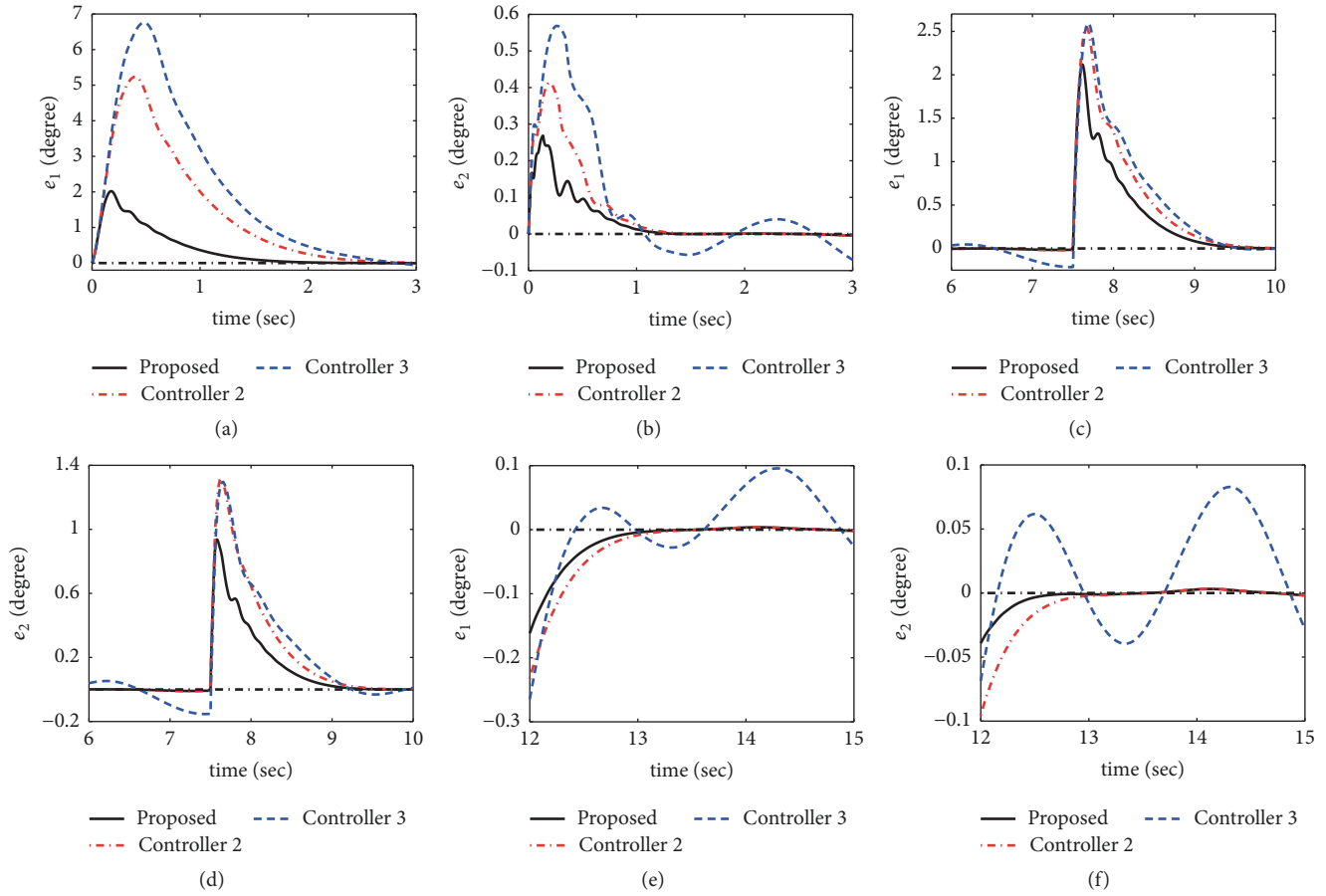


FIGURE 7: Simulation results of Case three: (a) and (b) are control errors within initial phase $t \in [1, 3]$ sec for joints 1 and 2, respectively; (c) and (d) are control errors within peak phase $t \in [6, 9]$ sec for joints 1 and 2, respectively; (e) and (f) are control errors within steady phase $t \in [12, 15]$ sec for joints 1 and 2, respectively.

TABLE 1: Initial and terminate points of the reference trajectory.

t (sec)	0.0	3.0	7.0	11.0	15.0
q_1 ($^\circ$)	0.0	30	-30	30	0.0
q_2 ($^\circ$)	0.0	30	-30	30	0.0

efforts enforcing the robot manipulator to accurately track the reference trajectory. Thanks to this mechanism, higher control accuracy and faster convergence have been clearly observed with our proposed method compared with the other twos.

Generally speaking, the effectiveness and advantages of our newly proposed method have been clearly demonstrated through the above comparative simulation studies. Higher control accuracy, faster dynamic response, and stronger robustness have been obviously observed in the simulation results.

5. Conclusions

For the high performance trajectory tracking control purpose of robot manipulators under complex lumped disturbance, a novel TDC scheme with ANTSM dynamics is proposed

and studied in this paper. The proposed method uses TDC as its basic control framework and brings in a fascinating model-free feature. Afterwards, a combined reaching law is used which combines the well-known fast-TSM-type reaching law with a constant reaching law using adaptive mechanism. Then, the TDC scheme is effectively enhanced with a designed NTSM surface and a combined reaching law. Thanks to this combined reaching law, higher control accuracy and faster dynamic response can be ensured with our proposed method compared with the existing methods. Stability of the closed-loop control system is analyzed using the Lyapunov method. Comparative simulations results show that our proposed TDC scheme with ANTSM dynamics can provide higher control accuracy, faster dynamic response, and better robustness against lumped disturbance than the two existing TDC schemes with NTSM dynamics.

Data Availability

The data used to support the findings of this study are available from the corresponding author upon request.

Conflicts of Interest

The authors declare no conflicts of interest.

Acknowledgments

This work was supported by the National Natural Science Foundation of China (51705243, 51805317), Natural Science Foundation of Jiangsu Province (BK20170789), China Postdoctoral Science Foundation (2018M630552).

References

- [1] Y. Wang, L. Gu, B. Chen, and H. Wu, "A new discrete time delay control of hydraulic manipulators," *Proceedings of the Institution of Mechanical Engineers, Part I: Journal of Systems and Control Engineering*, vol. 231, no. 3, pp. 168–177, 2017.
- [2] M. Jin, S. H. Kang, and P. H. Chang, "Robust compliant motion control of robot with nonlinear friction using time-delay estimation," *IEEE Transactions on Industrial Electronics*, vol. 55, no. 1, pp. 258–269, 2008.
- [3] M. Jin, S. H. Kang, P. H. Chang, and J. Lee, "Robust Control of Robot Manipulators Using Inclusive and Enhanced Time Delay Control," *IEEE/ASME Transactions on Mechatronics*, vol. 22, no. 5, pp. 2141–2152, 2017.
- [4] J. Baek, M. Jin, and S. Han, "A new adaptive sliding-mode control scheme for application to robot manipulators," *IEEE Transactions on Industrial Electronics*, vol. 63, no. 6, pp. 3628–3637, 2016.
- [5] Y. Wang, L. Gu, Y. Xu, and X. Cao, "Practical tracking control of robot manipulators with continuous fractional-order nonsingular terminal sliding mode," *IEEE Transactions on Industrial Electronics*, vol. 63, no. 10, pp. 6194–6204, 2016.
- [6] L. Zhang, L. Liu, Z. Wang, and Y. Xia, "Continuous finite-time control for uncertain robot manipulators with integral sliding mode," *IET Control Theory & Applications*, vol. 12, no. 11, pp. 1621–1627, 2018.
- [7] C. Yang, Y. Jiang, W. He, J. Na, Z. Li, and B. Xu, "Adaptive parameter estimation and control design for robot manipulators with finite-time convergence," *IEEE Transactions on Industrial Electronics*, vol. 65, no. 10, pp. 8112–8123, 2018.
- [8] G. P. Incremona, A. Ferrara, and L. Magni, "MPC for robot manipulators with integral sliding modes generation," *IEEE/ASME Transactions on Mechatronics*, vol. 22, no. 3, pp. 1299–1307, 2017.
- [9] B. Baigzadehnoe, Z. Rahmani, A. Khosravi, and B. Rezaie, "On position/force tracking control problem of cooperative robot manipulators using adaptive fuzzy backstepping approach," *ISA Transactions*, vol. 70, pp. 432–446, 2017.
- [10] R.-J. Wai and Z.-W. Yang, "Adaptive fuzzy neural network control design via a T-S fuzzy model for a robot manipulator including actuator dynamics," *IEEE Transactions on Systems, Man, and Cybernetics, Part B: Cybernetics*, vol. 38, no. 5, pp. 1326–1346, 2008.
- [11] S. Wang, J. Na, and X. Ren, "RISE-based asymptotic prescribed performance tracking control of nonlinear servo mechanisms," *IEEE Transactions on Systems, Man, and Cybernetics: Systems*, vol. 48, no. 12, pp. 2359–2370, 2018.
- [12] S. Wang, X. Ren, J. Na, and T. Zeng, "Extended-state-observer-based funnel control for nonlinear servomechanisms with prescribed tracking performance," *IEEE Transactions on Automation Science and Engineering*, vol. 14, no. 1, pp. 98–108, 2017.
- [13] S. Wang, J. Na, X. Ren, H. Yu, and J. Yu, "Unknown input observer-based robust adaptive funnel motion control for nonlinear servomechanisms," *International Journal of Robust and Nonlinear Control*, vol. 28, no. 18, pp. 6163–6179, 2018.
- [14] T. C. Steve Hsia, T. A. Lasky, and Z. Guo, "Robust Independent Joint Controller Design for Industrial Robot Manipulators," *IEEE Transactions on Industrial Electronics*, vol. 38, no. 1, pp. 21–25, 1991.
- [15] T. C. S. Hsia, "New technique for robust control of servo systems," *IEEE Transactions on Industrial Electronics*, vol. 36, no. 1, pp. 1–7, 1989.
- [16] K. Youcef-Toumi and O. Ito, "Time delay controller for systems with unknown dynamics," *Journal of Dynamic Systems, Measurement and Control*, vol. 112, no. 1, pp. 133–142, 1990.
- [17] M. Jin, J. Lee, P. H. Chang, and C. Choi, "Practical nonsingular terminal sliding-mode control of robot manipulators for high-accuracy tracking control," *IEEE Transactions on Industrial Electronics*, vol. 56, no. 9, pp. 3593–3601, 2009.
- [18] J. Lee, M. Jin, and K. K. Ahn, "Precise tracking control of shape memory alloy actuator systems using hyperbolic tangential sliding mode control with time delay estimation," *Mechatronics*, vol. 23, no. 3, pp. 310–317, 2013.
- [19] J. Kim, H. Joe, S.-C. Yu, J. S. Lee, and M. Kim, "Time-Delay Controller Design for Position Control of Autonomous Underwater Vehicle under Disturbances," *IEEE Transactions on Industrial Electronics*, vol. 63, no. 2, pp. 1052–1061, 2016.
- [20] J. Kim, P. Chang, and M. Jin, "Fuzzy PID controller design using time-delay estimation," *Transactions of the Institute of Measurement and Control*, vol. 39, no. 9, pp. 1329–1338, 2016.
- [21] J. Baek, S. Cho, and S. Han, "Practical Time-Delay Control with Adaptive Gains for Trajectory Tracking of Robot Manipulators," *IEEE Transactions on Industrial Electronics*, vol. 65, no. 7, pp. 5682–5692, 2018.
- [22] S. Roy, I. N. Kar, J. Lee, and M. Jin, "Adaptive-Robust Time-Delay Control for a Class of Uncertain Euler-Lagrange Systems," *IEEE Transactions on Industrial Electronics*, vol. 64, no. 9, pp. 7109–7119, 2017.
- [23] J. Lee, P. H. Chang, and M. Jin, "Adaptive integral sliding mode control with time-delay estimation for robot manipulators," *IEEE Transactions on Industrial Electronics*, vol. 64, no. 8, pp. 6796–6804, 2017.
- [24] M. Jin, J. Lee, and N. G. Tsagarakis, "Model-free robust adaptive control of humanoid robots with flexible joints," *IEEE Transactions on Industrial Electronics*, vol. 64, no. 2, pp. 1706–1715, 2017.
- [25] M. Jin, J. Lee, and K. K. Ahn, "Continuous nonsingular terminal sliding-mode control of shape memory alloy actuators using time delay estimation," *IEEE/ASME Transactions on Mechatronics*, vol. 20, no. 2, pp. 899–909, 2015.
- [26] B. Brahmi, M. Saad, C. Ochoa Luna, M. H. Rahman, and A. Brahmi, "Adaptive tracking control of an exoskeleton robot with uncertain dynamics based on estimated time delay control," *IEEE/ASME Transactions on Mechatronics*, vol. 23, no. 2, pp. 575–585, 2018.

- [27] S. Kim and J. Bae, "Force-mode control of rotary series elastic actuators in a lower extremity exoskeleton using model-inverse time delay control," *IEEE/ASME Transactions on Mechatronics*, vol. 22, no. 3, pp. 1392–1400, 2017.
- [28] R. Prasanth Kumar, A. Dasgupta, and C. S. Kumar, "Robust trajectory control of underwater vehicles using time delay control law," *Ocean Engineering*, vol. 34, no. 5-6, pp. 842–849, 2007.
- [29] R. P. Kumar, C. S. Kumar, D. Sen, and A. Dasgupta, "Discrete time-delay control of an autonomous underwater vehicle: Theory and experimental results," *Ocean Engineering*, vol. 36, no. 1, pp. 74–81, 2009.
- [30] F. Yan, Y. Wang, W. Xu, and B. Chen, "Time delay control of cable-driven manipulators with artificial bee colony algorithm," *Transactions of the Canadian Society for Mechanical Engineering*, vol. 42, no. 2, pp. 177–186, 2018.
- [31] Y. Wang, L. Gu, M. Gao, and K. Zhu, "Multivariable output feedback adaptive terminal sliding mode control for underwater vehicles," *Asian Journal of Control*, vol. 18, no. 1, pp. 247–265, 2016.
- [32] Y. Wang, F. Yan, B. Tian, L. Gu, and B. Chen, "Nonsingular terminal sliding mode control of underwater remotely operated vehicles," *Transactions of the Canadian Society for Mechanical Engineering*, vol. 42, no. 2, pp. 105–115, 2018.
- [33] Y. Wang, S. Jiang, B. Chen, and H. Wu, "A new continuous fractional-order nonsingular terminal sliding mode control for cable-driven manipulators," *Advances in Engineering Software*, vol. 119, pp. 21–29, 2018.
- [34] Y. Wang, F. Yan, S. Jiang, and B. Chen, "Time delay control of cable-driven manipulators with adaptive fractional-order nonsingular terminal sliding mode," *Advances in Engineering Software*, vol. 121, pp. 13–25, 2018.
- [35] G. Chen, B. Jin, and Y. Chen, "Nonsingular fast terminal sliding mode posture control for six-legged walking robots with redundant actuation," *Mechatronics*, vol. 50, pp. 1–15, 2018.
- [36] D. Qian and Y. Xi, "Leaderfollower formation maneuvers for multi-robot systems via derivative and integral terminal sliding mode," *Applied Sciences*, vol. 8, no. 7, pp. 1–16, 2018.
- [37] K. Wu, Z. Cao, J. Zhao, and Y. Wang, "Target Tracking Based on a Nonsingular Fast Terminal Sliding Mode Guidance Law by Fixed-Wing UAV," *Applied Sciences*, vol. 7, no. 4, pp. 1–18, 2017.
- [38] S. Yu, X. Yu, B. Shirinzadeh, and Z. Man, "Continuous finite-time control for robotic manipulators with terminal sliding mode," *Automatica*, vol. 41, no. 11, pp. 1957–1964, 2005.
- [39] H. Wang, L. Shi, Z. Man et al., "Continuous fast nonsingular terminal sliding mode control of automotive electronic throttle systems using finite-time exact observer," *IEEE Transactions on Industrial Electronics*, vol. 65, no. 9, pp. 7160–7172, 2018.
- [40] K. Liao and Y. Xu, "A Robust load frequency control scheme for power systems based on second-order sliding mode and extended disturbance observer," *IEEE Transactions on Industrial Informatics*, vol. 14, no. 7, pp. 3076–3086, 2018.
- [41] M. Li and Y. Chen, "Robust adaptive sliding mode control for switched networked control systems with disturbance and faults," *IEEE Transactions on Industrial Informatics*, 2018.
- [42] X. Cao, L. Gu, H. Qiu, C. Lai, and Y. Nan, "Continuous nonsingular terminal sliding mode contouring control of manipulator based on time delay estimation," *Proceedings of the Institution of Mechanical Engineers, Part I: Journal of Systems and Control Engineering*, vol. 231, no. 10, pp. 836–848, 2017.
- [43] Y. Wang, J. Chen, L. Gu, and X. Li, "Time delay control of hydraulic manipulators with continuous nonsingular terminal sliding mode," *Journal of Central South University*, vol. 22, no. 12, pp. 4616–4624, 2015.
- [44] Y. Wang, F. Yan, J. Chen, F. Ju, and B. Chen, "A new adaptive time-delay control scheme for cable-driven manipulators," *IEEE Transactions on Industrial Informatics*, 2018.
- [45] Z. Zhu, Y. Xia, and M. Fu, "Attitude stabilization of rigid spacecraft with finite-time convergence," *International Journal of Robust and Nonlinear Control*, vol. 21, no. 6, pp. 686–702, 2011.

